

Clonal hematopoiesis in angioimmunoblastic T-cell lymphoma with divergent evolution to myeloid neoplasms

Natasha E. Lewis,¹ Kseniya Petrova-Drus,¹ Sarah Huet,¹ Zachary D. Epstein-Peterson,² Qi Gao,¹ Allison E. Sigler,¹ Jeeyeon Baik,¹ Neval Ozkaya,¹ Alison J. Moskowitz,² Anita Kumar,² Steven M. Horwitz,² Yanming Zhang,³ Maria E. Arcila,⁴ Ross L. Levine,⁵⁻⁷ Mikhail Roshal,¹ Ahmet Dogan,^{1,*} and Wenbin Xiao^{1,5,7,*}

¹Hematopathology Service, Department of Pathology, ²Lymphoma Service, Department of Medicine, ³Cytogenetic Laboratory, Department of Pathology, ⁴Molecular Diagnostic Laboratory, Department of Pathology, ⁵Molecular Cancer Medicine Service, Human Oncology and Pathogenesis Program, ⁶Leukemia Service, Department of Medicine, and ⁷Center for Hematologic Malignancies, Memorial Sloan Kettering Cancer Center, New York, NY

Key Points

- CH is prevalent in patients with angioimmunoblastic T-cell lymphoma.
- Divergent clonal evolution of CH leads to therapy-related MNs in angioimmunoblastic T-cell lymphoma patients.

TET2 and *DNMT3A* mutations are frequently identified in T-cell lymphomas of T follicular helper cell origin (TCL-TFH), clonal hematopoiesis (CH), and myeloid neoplasms (MNs). The relationships among these 3 entities, however, are not well understood. We performed comprehensive genomic studies on paired bone marrow and tissue samples as well as on flow cytometry–sorted bone marrow and peripheral blood subpopulations from a cohort of 22 patients with TCL-TFH to identify shared CH-type mutations in various hematopoietic cell compartments. Identical mutations were detected in the neoplastic T-cell and myeloid compartments of 15 out of 22 patients (68%), including *TET2* (14/15) and *DNMT3A* (10/15). Four patients developed MNs, all of which shared CH-type mutations with their TCL-TFH; additional unique genetic alterations were also detected in each patient's TCL-TFH and MN. These data demonstrate that CH is prevalent in patients with TCL-TFH and that divergent evolution of a CH clone may give rise to both TCL-TFH and MNs.

Introduction

Angioimmunoblastic T-cell lymphoma (AITL) and nodal peripheral T-cell lymphoma with T follicular helper phenotype (PTCL-TFH) (both will be referred to as AITL hereafter) are aggressive lymphomas,¹ which frequently harbor mutations in the epigenetic modifiers *TET2*, *DNMT3A*, and *IDH2* and the small GTPase *RHOA*.²⁻¹⁰ *TET2* and *DNMT3A* mutations are also common in clonal hematopoiesis (CH)¹¹⁻¹⁴ and myeloid neoplasms (MNs).¹⁵⁻¹⁷ It has been hypothesized that *TET2* and *DNMT3A* mutations in AITL originate in hematopoietic stem/progenitor cells (HSPCs), which is supported by a few reports identifying these mutations in myeloid-derived cells of AITL patients.^{7,18-20} However, the relationships among CH, AITL, and MNs are not well understood. Herein, through comprehensive genomic evaluation of paired tissue and bone marrow (BM) samples as well as flow cytometry (FC)–sorted BM and peripheral blood (PB) subpopulations from a cohort of patients with AITL, we present compelling evidence that CH is prevalent in AITL patients and that it can divergently evolve to AITL and MNs.

Materials and methods

Patient and specimen selection

Patients with pathologically confirmed AITL or PTCL-TFH diagnosed between January 2011 and July 2019 as well as paired tissue involved by AITL and BM samples and/or FC-sorted BM samples available

Submitted 10 February 2020; accepted 23 April 2020; published online 22 May 2020.
DOI 10.1182/bloodadvances.2020001636.

*A.D. and W.X. contributed equally to this study.

Presented in poster form at the 12th annual T-Cell Lymphoma Forum, La Jolla, CA, 30-31 January 2020.

Original data are available from the corresponding author upon request.
The full-text version of this article contains a data supplement.

Table 1. Clinical characteristics of 22 patients with AITL

Patient	Sex	Age, y	Prior cancer history (treatment, dates)	Date of AITL diagnosis	Tissue used for NGS	BM bx date	Indication for BM bx	MN diagnosed on BM bx (type)	AITL-directed therapy prior to BM bx	Outcome	Overall survival, mo*
1	M	61	None	11/12/15	LN	8/29/17	Worsening anemia, TCP on chemo that persisted 2 mo after completion	No	Chemo, ASCT, localized XRT	DOD	22
2†	M	72	Prostate ca (XRT, 2015), smoldering MM (observation, 2016)	7/12/17	NA (NGS performed on FC sorted abnormal T cells from staging BM bx on 7/18/17)	8/28/19	New anemia, TCP 1.75 y after completion of chemo	Yes (MDS-SLD)	Chemo	DOD; progressed to MDS-EB-2	28
3	F	75	None	4/2/15	LN	1/14/16	Restaging at relapse	No	Chemo	DOD	12
4†	M	67	None	5/4/11	LN	9/19/11	End of treatment bx	No	Chemo	DOD	54
5†	F	68	Breast ca (chemo, XRT, hormonal therapy, 1997 and 2000)	12/23/15	Mesenteric mass	5/15/17	Evaluate disease status at relapse	No	Chemo	DOD	46
6†	F	73	None	3/4/15	LN	3/20/15	Initial staging	No	None	DOD	37
7†	M	44	None	8/9/17	Subcutaneous mass	9/15/17	Initial staging	No	None	A w/o active D	27
8†	F	82	None	8/8/14	LN	12/18/15	Acutely worsening pancytopenia 12 mo after completion of chemo	No	Chemo	AWD	63
9†	M	53	None	11/20/14	Skin	10/5/16	Persistent TCP 17 mo after completion of chemo	No	Chemo	DOD	41
10†	F	63	None	4/20/16	LN	12/10/18	Persistent pancytopenia 6 mo after ASCT	Yes (AML)	Chemo, ASCT	DOD	33
11†	M	71	None	3/23/15	LN	12/10/18	Worsening pancytopenia on clinical trial that persisted 1.75 mo after therapy cessation	Yes (MDS-EB-1)	Chemo	A w/o D; progressed to AML	56
12	M	69	None	8/7/18	LN	11/2/18	Repeat after possibility of MN raised on outside initial staging BM bx	No	Chemo	A w/o active D	15
13†	M	74	None	7/16/19	LN	7/30/19	Initial staging	No	None	AWD	4
14	F	61	Classical Hodgkin lymphoma (chemo, XRT, 2007)	12/7/11	LN	1/5/18	Confirm relapse	No	Chemo, ASCT, TT	A w/o D	95
15†	F	81	None	6/10/14	LN	6/13/14	Initial staging	No	None	A w/o active D	65
16	M	73	Prostate ca (active surveillance then resection in 2017)	2/19/15	LN	3/4/15	Initial staging	No	None	A w/o D	57
17†	F	69	None	8/11/11	Skin	3/16/18	Persistent cytopenias 18 mo after relapse (on therapy) and assess disease status at first visit to our institution	No	Chemo, ASCT	AWD	98
18	M	71	Clear cell RCC (excision, 2004; recurrence/metastasis, observed since 2012)	3/5/15	LN	3/2/18	Staging of newly diagnosed laryngeal plasmacytoma	No	Chemo	A w/o D	57
19	M	67	None	7/12/17	LN	8/8/17	Initial staging	No	None	DOD	7

A w/o D, alive without evidence of disease (AITL); AML, acute myeloid leukemia; ASCT, autologous stem cell transplant; AWD, alive with disease (AITL); bx, biopsy; ca, cancer; chemo, chemotherapy; CMML-0, chronic myelomonocytic leukemia 0; DLBCL, diffuse large B-cell lymphoma; DOD, dead of disease; F, female; LAD, lymphadenopathy; LN, lymph node; M, male; MDS-EB-1, myelodysplastic syndrome with excess blasts 1; MDS-EB-2, myelodysplastic syndrome with excess blasts 2; MDS-SLD, myelodysplastic syndrome with single lineage dysplasia; MM, multiple myeloma; NA, not applicable; RCC, renal cell carcinoma; TCP, thrombocytopenia; TT, targeted therapy; XRT, radiation.

*Overall survival indicates the time from AITL diagnosis to date of death or last follow-up.
†Patients with evidence of shared mutations in their AITL and non-AITL BM compartment.

Table 1. (continued)

Patient	Sex	Age, y	Prior cancer history (treatment, dates)	Date of AITL diagnosis	Tissue used for NGS	BM bx date	Indication for BM bx	MN diagnosed on BM bx (type)	AITL-directed therapy prior to BM bx	Outcome	Overall survival, mo*
20†	M	93	Melanoma (excision, 2016)	11/30/17	NA (NGS performed on FC sorted abnormal T-cells from staging BM bx on 12/22/17)	12/22/17	Initial staging	No	None	AWD	19
21†	M	66	Bladder ca (excision, date unknown)	12/19/14	Spleen	1/8/18	Required for clinical trial enrollment at time of relapse	No	Chemo, TT	AWD	59
22†	M	73	None	9/30/16	LN	7/11/19	Required for clinical trial enrollment at time of relapse	Yes (CMML-0)	Chemo, ASCT	A w/o active D; persistent CMML	37

A w/o D, alive without evidence of disease (AITL); AML, acute myeloid leukemia; ASCT, autologous stem cell transplant; AWD, alive with disease (AITL); bx, biopsy; ca, cancer; chemo, chemotherapy; CMML-0, chronic myelomonocytic leukemia 0; DLBCL, diffuse large B-cell lymphoma; DOD, dead of disease; F, female; LAD, lymphadenopathy; LN, lymph node; M, male; MDS-EB-1, myelodysplastic syndrome with excess blasts 1; MDS-EB-2, myelodysplastic syndrome with excess blasts 2; MDS-SLD, myelodysplastic syndrome with single lineage dysplasia; MM, multiple myeloma; NA, not applicable; RCC, renal cell carcinoma; TCP, thrombocytopenia; TT, targeted therapy; XRT, radiation.

*Overall survival indicates the time from AITL diagnosis to date of death or last follow-up.
†Patients with evidence of shared mutations in their AITL and non-AITL BM compartment.

for targeted next-generation sequencing (NGS) were identified. All cases were independently reviewed by at least 2 hematopathologists (N.E.L. and W.X.). Clinical data were obtained from electronic medical records. The study was approved by the Institutional Review Board of Memorial Sloan Kettering Cancer Center and written informed consent was obtained from all patients.

FC and cell sorting

Multiparameter FC analysis was performed on 21 of the 22 BM samples. Where live cells were available, FC cell sorting was performed on BM (n = 6) or PB (n = 3).

Cytogenetic and mutational analysis

Conventional karyotype, fluorescence in situ hybridization, and/or T-cell receptor (*TCR*) gene rearrangement analysis were performed on BMs during clinical workup. Targeted NGS-based mutational analysis was performed on tissues, BMs, and FC-sorted cells using various assays (supplemental Methods; supplemental Table 1). A droplet digital polymerase chain reaction assay was also performed on selected BM and PB samples (n = 4) (supplemental Table 1). Only mutations with variant allele frequencies (VAFs) of $\geq 2\%$ were included in our analysis. In non-FC-sorted BM samples, VAFs of mutations and percent involvement by AITL were compared to identify the cellular compartment in which a mutation was present (neoplastic T cells or myeloid compartment). Mutations were considered present in the BM myeloid compartment if their VAFs were ≥ 4 times the AITL percentage.

Statistical analysis

Overall and progression-free survival was evaluated using Kaplan-Meier analysis. Categorical variables were compared using Fisher's exact test.

Results

CH-type mutations are frequently shared in both neoplastic T cells and myeloid compartments among patients with AITL

We identified 71 patients with AITL or PTCL-TFH and with NGS analysis of diagnostic lymphoma samples, among which 64 (90%)

and 23 (32%) harbored *TET2* and *DNMT3A* mutations, respectively, consistent with the literature.^{5,6,8,9} All but 2 of the *DNMT3A*-mutated cases also carried *TET2* mutations. Twenty-two of the *TET2*-mutated patients had NGS studies previously performed on BM (n = 10) or had BM samples available for sequencing (n = 12). Of note, 1 patient was identified with a pathologically confirmed diagnosis of a myeloproliferative neoplasm (MPN) with a *JAK2* p.V617F mutation reportedly detected at an outside institution, which preceded development of AITL. However, as no BM or PB samples were available at our institution for sequencing, this case was excluded. Clinical characteristics of the cohort are described in Table 1. Sequencing of the AITLs (Figure 1A-B) identified mutations of *TET2* in 22 out of 22 cases (100%), *DNMT3A* in 13 out of 22 cases (59%), *RHOA* G17V in 12 out of 22 cases (55%), and *IDH2* R172 in 7 out of 22 cases (32%) (Figure 1D; Table 2; supplemental Figure 1; supplemental Table 2), a mutational profile characteristic of AITL.²⁻¹⁰

BM biopsies (Figure 1A-C) were performed at various time points (Figure 1E), most commonly for staging purposes (n = 12) or cytopenias after therapy (n = 7) (Table 1). No patient had a prior diagnosis of a MN. BMs from 10 patients showed various degrees of AITL involvement by morphology (5% to 50% in 7 out of 22 cases [32%] and $< 5\%$ in 3 out of 22 cases [14%]). The remaining 12 (55%) patients had no BM involvement morphologically, 3 of whom had measurable residual disease as detected by FC (0.0079% in patient 12 and 0.036% in patient 22) and/or *TCR* gene rearrangement analysis only (FC was negative in patient 7) (Figure 1A,D; supplemental Table 2).

Identical mutations were detected in the neoplastic T-cell and myeloid compartments of 15 (68%) patients, including *TET2* (14/15) and *DNMT3A* (10/15) mutations (Figure 1D,F-H; Table 2; supplemental Figure 1; supplemental Table 2), consistent with the hypothesis that a subset of AITL originates from a *TET2* and/or *DNMT3A*-mutated HSPC. The BMs from 9 patients had no morphologic involvement by AITL but were positive for *TET2* and/or *DNMT3A* mutations, with VAFs of 2.4% to 46.8% and 2.8% to 36.2%, respectively (Figure 1F-G; supplemental Table 2), suggesting myeloid origin. Indeed, FC

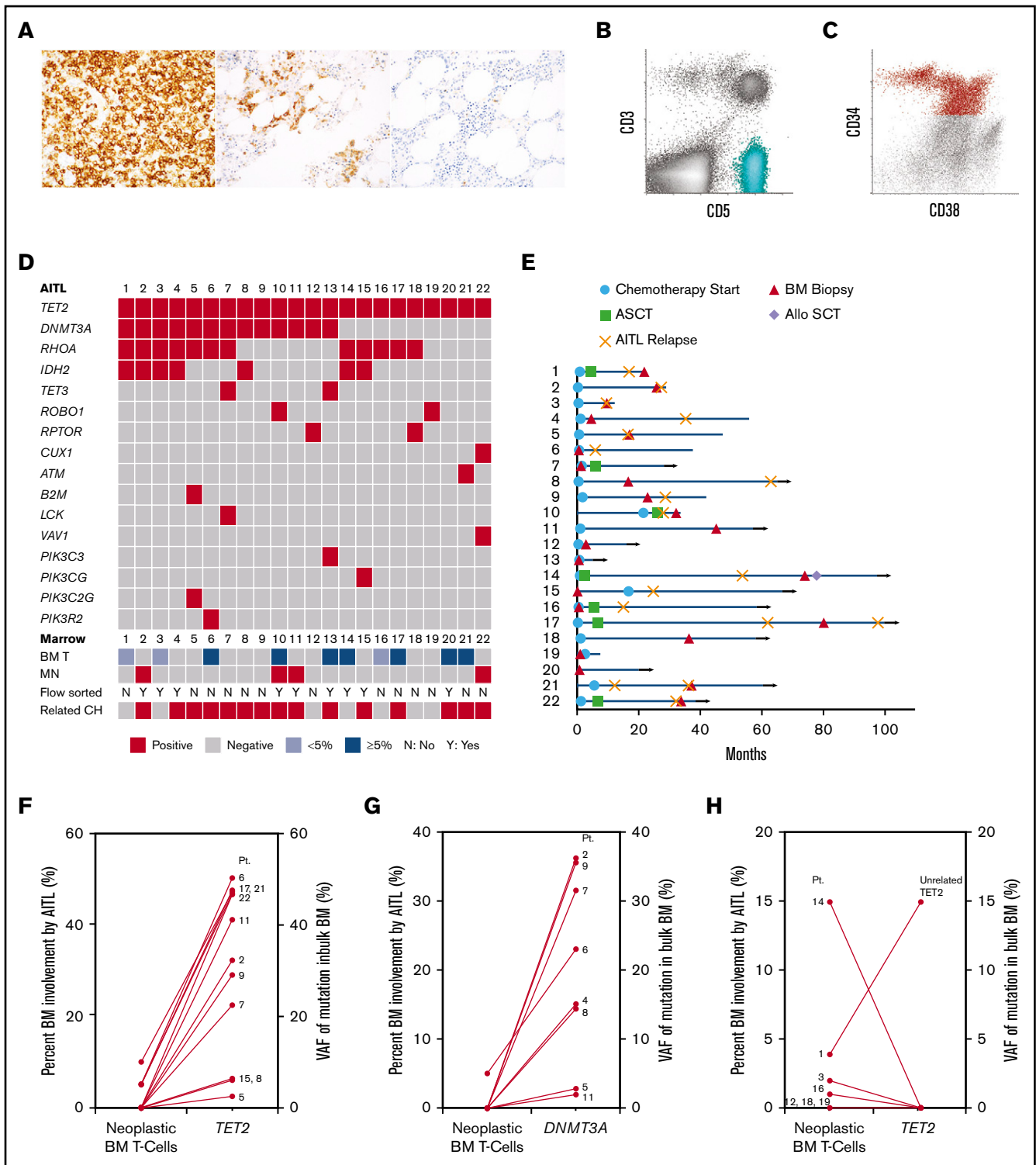


Figure 1. Histologic, flow cytometric, clinical and mutational features of 22 patients with AITL. (A) Photomicrographs of PD-1 immunohistochemical stains from 3 patients (original magnification $\times 400$). An example lymph node biopsy specimen from patient 16 (far left) demonstrates a proliferation of strongly PD-1-positive T cells, consistent with AITL. The middle image depicts a BM biopsy specimen from patient 14 with lymphohistiocytic aggregates containing PD-1-positive T cells, consistent with involvement by AITL. The far right image depicts a BM biopsy specimen from patient 11 that showed small lymphoid aggregates that were negative for PD-1, consistent with a reactive infiltrate, which was confirmed by FC. (B-C) Scatterplots from FC analyses of a BM involved by AITL (patient 17) (B, aqua neoplastic T-cell population) and a BM involved by MDS (patient 2) (C, red CD34⁺ abnormal myeloid blast population). (D) Mutations detected in the AITL of each patient (each column represents 1 patient and is annotated with the patient's identification number). The degree of AITL involvement in each patient's paired BM (BM T), as well as whether a MN was identified, whether FC sorting was performed, and if shared *TET2* and/or *DNMT3A* mutations were detected in the myeloid compartment (related CH), are also indicated in the bottom rows.

sorting of either BM or PB samples from 3 of the 9 patients (patients 4, 11, and 15) confirmed the mutations were present in the myeloid compartments (Table 2). Six patients had $\geq 5\%$ involvement by AITL in the BM by morphology, 3 of whom had *TET2* VAFs of $\sim 50\%$ (50.3% in patient 6, 47.6% in patient 17, and 47.4% in patient 21), > 4 times the percentage of neoplastic T cells (5% in patient 6, 5% in patient 17, 10% in patient 21) (Figure 1F; supplemental Table 2), inferring a myeloid origin. FC sorting of the BMs from the other 3 patients (patients 10, 13, and 20) confirmed the presence of identical *TET2* with or without *DNMT3A* mutations in both the neoplastic T cells and myeloid populations in all 3 patients and in normal B cells in 1 case (patient 13) (Figure 2A; Table 2). To confirm the accuracy of our NGS studies, we FC sorted PB samples from 2 patients with $< 5\%$ (patient 3) and 15% (patient 14) BM involvement by AITL and without evidence of shared mutations in the myeloid compartment based on VAFs from the bulk BM. We confirmed the presence of mutations in the sorted neoplastic T cells (patient 3) and not in the sorted myeloid cells (patients 3 and 14) (Table 2). Interestingly, patient 1, who died shortly after his BM biopsy, had unrelated *TET2*, *RUNX1*, and *SRSF2* mutations in the BM, indicative of an independent high-risk CH (Figure 1H; supplemental Figure 1 and Table 2). Only 2 additional shared variants were identified in 2 different patients. Patient 15 harbored a shared *PIK3CG* p.V74M variant, while patient 22 demonstrated a shared *CHEK2* p.D134G variant (supplemental Table 2). Both variants were likely somatic in nature based on the VAFs and occurred in the early clone. While these variants may play important roles in oncogenesis, including in T-cell lymphoma and MNs,²¹⁻²³ whether they represented passenger or driver mutations is unclear. *RHOA* and *IDH2* mutations identified in the lymphomas were not detected in the corresponding myeloid compartments (Table 2; supplemental Table 2).

No difference in overall survival was seen between patients with and without CH (supplemental Figure 2). A trend toward improved progression-free survival was observed in patients without CH (median not reached vs 41 months, $P = .025$). Only 2 of 16 patients with CH (including patient 1 with unrelated CH) had no evidence of disease (AITL or MN) at last follow-up compared with 4 of 6 patients without CH ($P = .025$).

MNs in AITL patients result from divergent evolution of an early CH clone

Patients 2, 10, 11, and 22 subsequently developed MDS with a complex karyotype (including -7), AML (Figure 3), MDS-EB-1 (which progressed to AML within 6 months), and CMML-0, respectively, 2, 2.7, 3.6, and 2.7 years after their AITL diagnoses, respectively. All 4 patients shared identical CH-type mutations in their AITL and MN, including multiple *TET2* mutations in 4 out of 4 patients and single *DNMT3A* mutations in 3 out of 3 patients with *DNMT3A*-mutated AITL, suggesting both malignancies

arose from early clones harboring multiple CH-type mutations. The AITLs and MNs in all 4 patients also harbored multiple additional differing alterations that were not shared between them (Figure 2B-F).

A PB sample from patient 2 obtained soon after his initial AITL diagnosis (~ 2 weeks after his initial staging BM biopsy), prior to AITL-directed chemotherapy (and ~ 2 years prior to his MDS diagnosis), demonstrated the same *DNMT3A* and 2 *TET2* mutations as those detected in his AITL and MDS at relatively low VAFs (7%, 5%, and 5%, respectively). A concurrent FC analysis of that PB sample demonstrated an abnormal T-cell population that comprised 0.96% of the total white cells. As the VAFs of the *DNMT3A* and *TET2* mutations were much greater (> 4 times) than the percentage of circulating neoplastic T cells in this PB sample, it suggests these mutations were present in cellular compartments outside the AITL and is indicative of a low-level CH clone. At the time of MDS diagnosis, the VAFs had increased to 30% to 40%, consistent with a growth advantage conferred by these mutations under pressure of chemotherapy.

Discussion

Although this retrospective study has some selection bias, through comprehensive evaluation of the largest cohort of AITL patients to date using sensitive and accurate FC and genotyping techniques as well as FC sorting of a relatively large number of BM/PB samples, we demonstrate that AITL patients frequently harbor *TET2* and *DNMT3A* mutant alleles in both neoplastic T-cell and myeloid compartments, confirming the findings of prior case studies.^{3,7,8} Additionally, using FC sorting of both neoplastic T cells and neoplastic myeloid populations, we identified identical *TET2* with or without *DNMT3A* mutations in the AITLs and MNs of all 4 patients who developed MN, indicating both malignancies arose from a common *TET2* with or without *DNMT3A*-mutated CH clone, as well as differing sets of genomic alterations in each neoplasm. Our data suggest that *TET2* and *DNMT3A* mutations occur in HSPCs with the potential to clonally evolve to AITL and MN, which is driven by additional and divergent genetic events. Among patients without MNs, the sizes of the related CH clones in our cohort varied widely, from $\sim 2\%$ to $\sim 50\%$. In addition, the CH clones often harbored ≥ 2 *TET2* mutations (10 out of 15 [67%]) and/or both *TET2* and *DNMT3A* mutations (9 out of 15 [60%]), which is more frequent than in the general population with CH (multiple mutations reported in $\sim 5\%$ to 15%).^{11,12,24,25} The significance of CH with multiple mutations is unclear but may be associated with an increased risk of therapy-related MN.²⁶ Overall, this pathobiology may place AITL patients at higher risk of MN, especially after chemotherapy, which may have important management and therapeutic implications.

Kommalapati et al²⁷ evaluated the occurrence of AML after the diagnosis of AITL using Surveillance, Epidemiology, and End

Figure 1. (continued) (E) Swimmer plot indicating the time points at which the sequenced BM biopsy was obtained, chemotherapy was initiated, or autologous or allogeneic stem cell transplant (ASCT or Allo SCT, respectively) was performed, as well as points of AITL relapse for each patient (each row represents 1 patient and is annotated with the patient's identification number). Month 0 indicates the time at which AITL was first diagnosed. Horizontal arrows indicate patients alive at last follow-up. (F-G) Comparison of the level of BM involvement by AITL (neoplastic BM T cells) to the VAFs of the *TET2* and *DNMT3A* mutations detected in the sequenced bulk BMs among patients with shared *TET2* (F) and *DNMT3A* (G) mutations. (H) Patients without shared *TET2* mutations. Each line represents one patient and is annotated with the corresponding patient identification number.

Table 2. Genotyping analysis of FC sorted BM and PB subpopulations from 9 patients

	Genetic alterations	Sorted populations		
		VAF in abnormal T cells	VAF in abnormal plasma cells	
Patient 2†	DNMT3A p.R736C	0.478	0	
	TET2 p.Q810*	0.463	0	
	TET2 p.Y1128*	0.458	0	
	IDH2 p.R172K	0.406	0	
	RHOA p.G17V	0.459	0	
	ATR p.D1409N	0.206	0	
	KMT2B p.Q757*	0.248	0	
	BRCA2 p.A2306S	0	0.478	
	BTG1 p.K29*	0	0.484	
	EPHA5 p.G1033E	0	0.229	
	KMT2D p.H1525Pfs*37	0	0.248	
	SETD5 p.Y987F	0	0.345	
Patient 3†‡		VAF in abnormal T cells	VAF in monocytes	
	TET2 p.Y592fs	0.505	0.005	
	DNMT3A exon11 splicing variant (c.1279+1G>A)	0.473	0.003	
	IDH2 p.R172K	0.489	0.002	
		0.479	0.001	
Patient 4†‡		VAF in abnormal T cells	VAF in monocytes	
	TET2 p.Y1337*	0.550	0	
	DNMT3A p.W795C	0.488	0.065	
	IDH2 p.R172G	0	0	
		0.491	0	
Patient 10		VAF in abnormal T cells	VAF in abnormal CD34 ⁺ myeloid blasts	VAF in monocytes
	TET2 p.C1289Y	0.506	0.481	0.478
	TET2 p.L1899Sfs*9	0.446	0.32	0.542
	DNMT3A p.R771*	0.51	0.4	0.514
	DNMT3A p.C861Y	0	0.406	0.359
	RUNX1 p.A329Sfs*271	0	0.621	0.423
	ARID1B p.S914N	0.349	0	0
	DDX3X p.V526A	0.234	0	0
	NFE2 p.T318A	0.341	0	0
ROBO1 p.G904R	0.516	0	0	
Patient 11		VAF in abnormal CD34 ⁺ myeloid blasts	VAF in abnormal CD117 ⁺ /CD34 ⁻ blasts	VAF in normal lymphocytes
	TET2 p.C484fs	0.128	0.394	0.148
	TET2 p.L757fs	0.196	0.463	0.139
	DNMT3A p.I471*	0.180	0	0.009
	EPHA5 p.D136N	0	0	0
	WT1 p.S189*	0	0.371	0
WT1 p.S71Lfs*128	0	0.029	0	

*stop codon mutation.

†Flow-sorted BM or PB samples that are different from the BM samples described in Table 1 and supplemental Figure 1 and Table 2. The BM sample from patient 2 reported in this table was obtained at the time of initial AITL diagnosis while the BM sample reported in Table 1 and supplemental Figure 1 and Table 2 was obtained ~2 years later at the time of MDS diagnosis. The sample reported in this table from patient 3 is a PB sample obtained at the time of initial AITL diagnosis, while the BM sample reported in Table 1 and supplemental Figure 1 and Table 2 was obtained <1 year later at the time of AITL relapse. The sample reported in this table from patient 4 is a BM sample obtained at the time of AITL relapse, while the BM sample reported in Table 1 and supplemental Figure 1 and Table 2 was obtained ~2.5 years earlier after completion of the first round of AITL-directed chemotherapy. The sample reported in this table from patient 14 is a PB sample obtained at the time of first AITL relapse, while the BM sample reported in Table 1 and supplemental Figure 1 and Table 2 was obtained <1 year later at the time of second AITL relapse. The sample reported in this table from patient 15 is a PB sample obtained during routine surveillance, while the BM sample reported in Table 1 and supplemental Figure 1 and Table 2 was obtained ~3 years prior at initial AITL diagnosis.

‡Samples that were genotyped using droplet digital polymerase chain reaction.

Table 2. (continued)

Genetic alterations	Sorted populations		
	VAF in abnormal T cells	VAF in abnormal plasma cells	
Patient 13	VAF in abnormal T cells	VAF in normal myeloid cells	VAF in normal B cells
DNMT3A p.K455*	0.485	0.375	0.206
TET2 p.G641W	0.465	0.085	0.196
TET2 p.S631*	0.477	0.084	0.198
TET2 p.Q1030*	0	0.250	0
SF3B1 p.K700E	0	0.205	0
TET2 p.V1232Gfs*21	0	0	0.11
TET3 p.C695Y	0.502	0	0
TET3 p.C693G	0.475	0	0
Patient 14†‡	VAF in monocytes		
TET2 p.C973fs	0		
TET2 p.R1216*	0		
IDH2 p.R172S	0		
RHOA p.G17V	0		
Patient 15†‡	VAF in monocytes		
TET2 p.570fs	0.22		
IDH2 p.R172G	0		
RHOA p.G17V	0		
Patient 20	VAF in abnormal T cells	VAF in granulocytes	
TET2 p.R1440Tfs*38	0.689	0.327	
TET2 p.S794*	0.045	0.294	
TET2 p.W1003*	0.011	0.079	
TET2 p.H850Qfs*19	0.005	0.038	
DNMT3A p.R736H	0.008	0.064	

*stop codon mutation.

†Flow-sorted BM or PB samples that are different from the BM samples described in Table 1 and supplemental Figure 1 and Table 2. The BM sample from patient 2 reported in this table was obtained at the time of initial AITL diagnosis while the BM sample reported in Table 1 and supplemental Figure 1 and Table 2 was obtained ~2 years later at the time of MDS diagnosis. The sample reported in this table from patient 3 is a PB sample obtained at the time of initial AITL diagnosis, while the BM sample reported in Table 1 and supplemental Figure 1 and Table 2 was obtained <1 year later at the time of AITL relapse. The sample reported in this table from patient 4 is a BM sample obtained at the time of AITL relapse, while the BM sample reported in Table 1 and supplemental Figure 1 and Table 2 was obtained ~2.5 years earlier after completion of the first round of AITL-directed chemotherapy. The sample reported in this table from patient 14 is a PB sample obtained at the time of first AITL relapse, while the BM sample reported in Table 1 and supplemental Figure 1 and Table 2 was obtained <1 year later at the time of second AITL relapse. The sample reported in this table from patient 15 is a PB sample obtained during routine surveillance, while the BM sample reported in Table 1 and supplemental Figure 1 and Table 2 was obtained ~3 years prior at initial AITL diagnosis.

‡Samples that were genotyped using droplet digital polymerase chain reaction.

Results program database data and reported a higher risk of subsequent development of AML than that of the general United States population (standard incidence ratio, 23.1 between 2 and 11 months, 36.5 between 1 and 10 years, and 49.6 after 10 years). As this study was limited to patients who only developed AML (and did not include other MNs) after being diagnosed with T-cell lymphomas, these data may underestimate the true prevalence of MNs in AITL patients. Despite the possibility of selection bias, 4 of the 22 patients in our cohort developed MNs, an alarmingly high incidence. Our study infers that AITL patients should be evaluated for CH and monitored for therapy-related MN, particularly those with CH.

Our study depicts a variety of types of related MNs in AITL patients, including MDS, AML and MDS/MPN, with variable cytogenetic alterations and mutations. Interestingly, all 4 patients in our cohort with both AITL and MNs developed the MN after being diagnosed and

treated for AITL with CHOP-based chemotherapy (cyclophosphamide, doxorubicin, and vincristine). In 3 of these patients, the MNs were discovered upon workup for cytopenias. Also of interest, all of the MNs in our cohort developed in a similar time frame of ~2-4 years after the AITL diagnosis and ~1-4 years after initiation of chemotherapy, typical of therapy-related MNs after topoisomerase II inhibitor (such as doxorubicin) therapy.²⁸ In fact, in one of these patients (patient 2), we show that the CH clone was likely present at a low level at the time of initial AITL diagnosis and expanded more than fourfold at the time of MDS development, possibly due to the selective pressure of the AITL-directed chemotherapy. While theoretically, if AITL and MNs arise from a common CH-like clone, one may expect to see a combination of patients who develop MNs both before and after the development of AITL. Although we did identify 1 patient with a *JAK2* V617F-positive MPN that preceded the diagnosis of AITL, no BM or PB samples were available for sequencing,

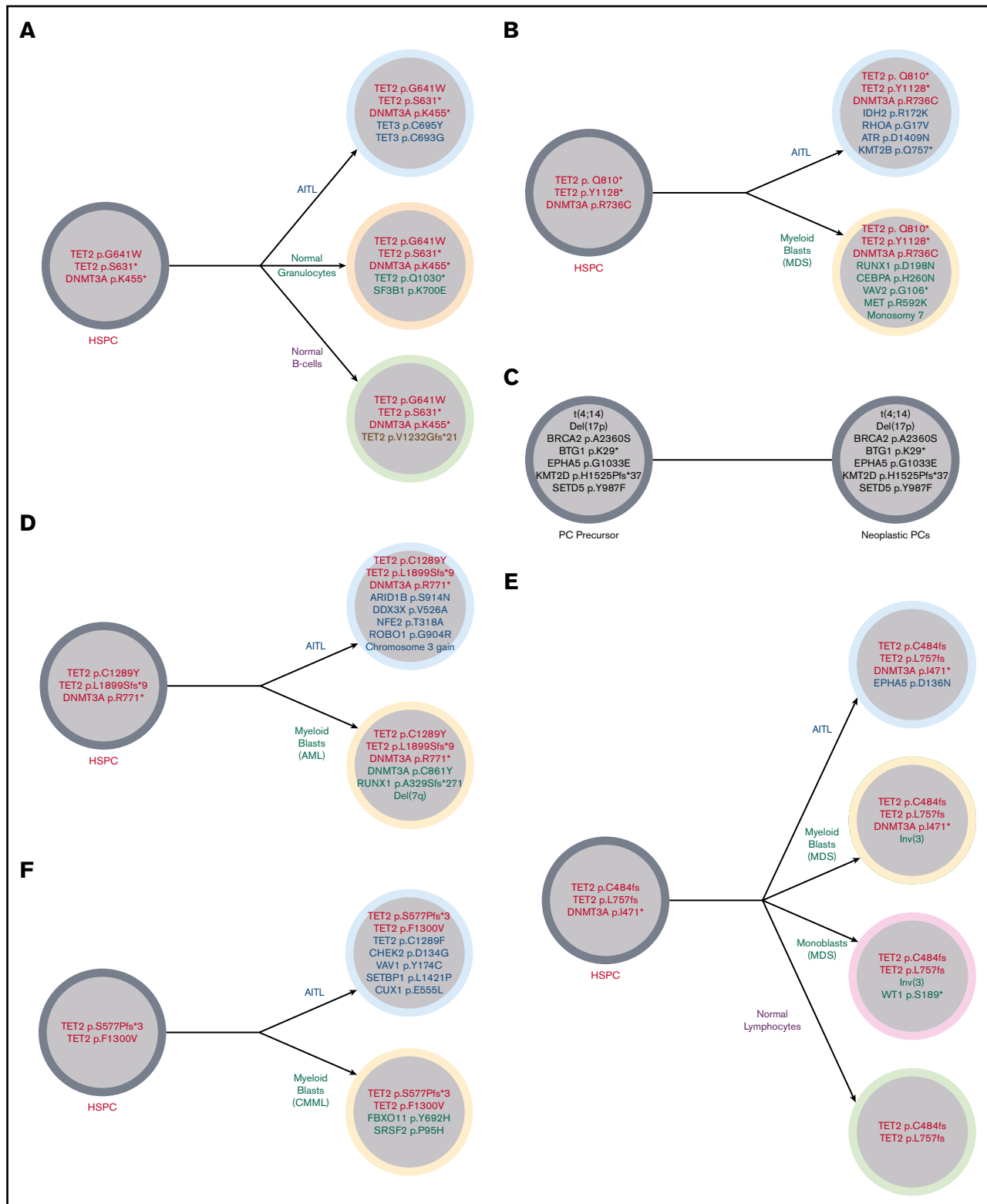


Figure 2. Illustration of the clonal architecture of hematopoietic cell populations from 5 patients. (A) Identical *TET2* and *DNMT3A* mutations were detected in the FC-sorted neoplastic T cells (AITL), normal granulocytes, and normal B cells from the BM of patient 13, suggesting origin of all populations from a shared HSPC precursor harboring *TET2* and *DNMT3A* mutations. This sequenced BM did not meet World Health Organization criteria for diagnosis of a MN. (B) Patient 2 developed MDS with a complex karyotype 2 years after being diagnosed with AITL. Identical *DNMT3A* and 2 *TET2* mutations were identified in the FC-sorted neoplastic T cells from the patient's original AITL staging BM (obtained 2 years prior to development of MDS) and the bulk BM obtained at the time of the MDS diagnosis (which showed no involvement by AITL), consistent with origin of both neoplasms from a common *TET2*- and *DNMT3A*-mutated HSPC precursor. Alterations limited to the AITL included *RHOA*, *IDH2*, *ATR*, and

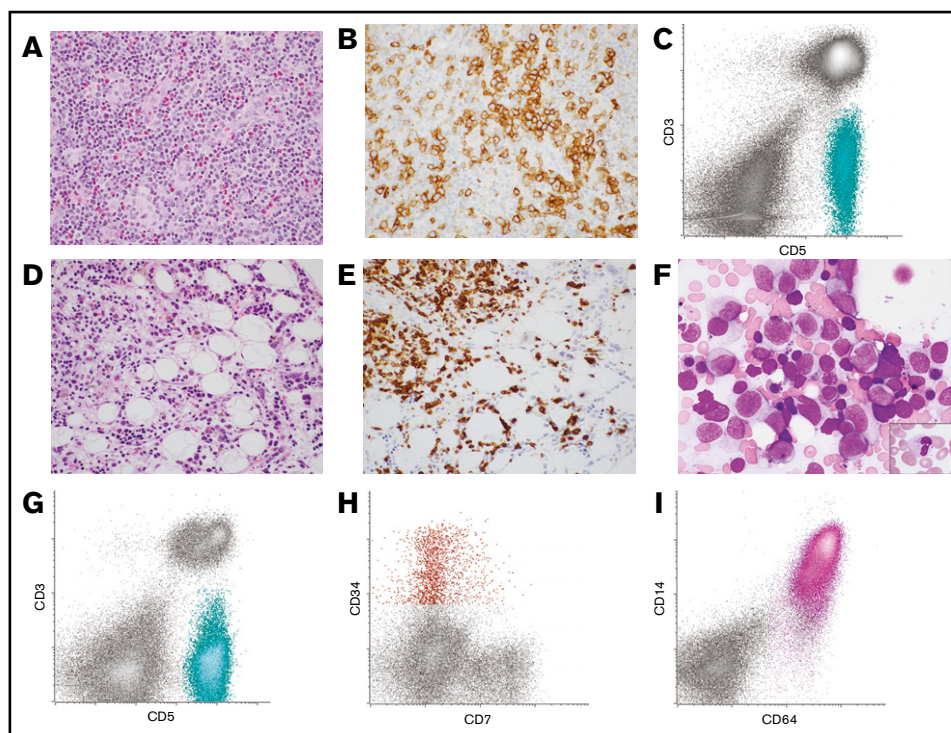


Figure 3. Lymph node and BM morphology with corresponding FC histograms from patient 10 with AITL and AML. (A-B) Lymph node was effaced by an infiltrate of small to intermediate-sized lymphoid cells with moderate amounts of pale cytoplasm in a background of mixed inflammatory cells and vascular proliferation (A, hematoxylin and eosin stain, original magnification $\times 400$). (B) The neoplastic T cells expressed PD-1 by immunohistochemistry (original magnification $\times 400$). (C) FC analysis of the lymph node demonstrated an abnormal T-cell population that was surface CD3(–) and CD5(+) (aqua population). These cells were also positive for CD4, CD2, and PD-1 (not shown). The findings were consistent with AITL. (D-F) Subsequent BM biopsy demonstrated aggregates of atypical lymphoid cells as well as increased blasts and promonocytes. (D) Hematoxylin and eosin–stained core biopsy, original magnification $\times 400$. (E) CD3 immunohistochemistry performed on the core biopsy specimen highlighted the neoplastic T cells (original magnification $\times 400$). (F) Wright-Giemsa–stained aspirate smear demonstrated frequent blasts/promonocytes as well as dysgranulopoiesis (inset) and dyserythropoiesis (original magnification $\times 1000$). (G-I) FC analysis of the BM detected a surface CD3(–), CD5(+) abnormal T-cell population similar to that seen in the lymph node (aqua population) (G) as well as a small abnormal CD34(+) myeloid blast population with dim CD7 expression (red population) (H) and an expanded CD64(+) monoblast population (pink population) (I). The findings were consistent with BM involvement by both AITL and AML with monocytic differentiation.

precluding evaluation of a clonal relationship between the neoplasms. A recent study also described patients with MPNs preceding AITL, but clonal relatedness was not shown.²⁹ In the literature, both patients with MNs preceding AITL^{3,7,18,20} and patients with MNs developing after AITL^{19,30} have been reported, although in only rare cases was a clonal link clearly demonstrated between the 2 neoplasms. Given that both

scenarios have been reported, it may be that due to our sample size, we only identified patients who developed MNs following their AITL with confirmed clonal relationships. However, we cannot exclude the possibility that this reflects the underlying biology of this disease, such as a unique type of CH with greater propensity for AITL. Additional study would be needed to better understand this result.

Figure 2. (continued) *KMT2B* mutations, while those limited to the MDS included *CEBPA* and *RUNX1* mutations, consistent with the acquisition of separate and divergent genomic events in each neoplasm. (C) Patient 2 also had a history of smoldering plasma cell (PC) myeloma diagnosed 14 months prior to his AITL. FC sorting of neoplastic T cells and plasma cells and fluorescence in situ hybridization analysis of enriched CD138⁺ plasma cells from his staging BM sample at the time of AITL diagnosis demonstrated differing sets of genetic alterations in each population, consistent with 2 unrelated neoplastic processes. (D) Patient 10 developed AML 2.7 years after his AITL diagnosis. FC-sorted leukemic myeloid blasts and neoplastic T cells from BM shared 2 *TET2* mutations and 1 *DNMT3A* mutation. Alterations limited to the AML included *del(7q)*, a *RUNX1* mutation, and an additional *DNMT3A* mutation, while the AITL harbored a number of mutations (including *ARID1B* and *ROBO1*) and gain of chromosome 3 not seen in the AML. (E) Patient 11 developed MDS-EB-1 3.6 years after being diagnosed with AITL. Bulk AITL tissue and FC-sorted neoplastic BM myeloid blasts shared 2 *TET2* mutations and 1 *DNMT3A* mutation; the same *TET2* mutations were also identified in FC-sorted normal lymphocytes. Alterations limited to the neoplastic myeloid population included an *inv(3)*, while only the neoplastic T cells had an *EPHA5* mutation. (F) Patient 22 developed CMML-0 2.7 years after being diagnosed with AITL. Comparison of VAFs from bulk BM (negative for AITL) and tissue samples demonstrated 2 shared *TET2* mutations in AITL and CMML. Only CMML harbored a *SRSF2* mutation, while the AITL harbored a number of additional mutations (including an additional *TET2* mutation) not identified in CMML. MDS, myelodysplastic syndrome.

Acknowledgments

This work was supported in part through the National Institutes of Health, National Cancer Institute cancer center support grant P30 CA008748. A.E.S. and A.D. are supported by a grant from the National Institutes of Health, National Cancer Institute (P50 CA192937).

Authorship

Contribution: N.E.L., M.R., A.D., and W.X. conceived the study, collected and analyzed the data, and wrote the manuscript; K.P.-D. annotated the sequencing data and wrote the manuscript; S.H., A.E.S., J.B., N.O., and M.E.A. collected data; Z.D.E.-P., A.J.M., A.K., and S.M.H. provided critical clinical information; Q.G. aided with flow cell sorting; Y.Z. reviewed the cytogenetic data; R.L.L. analyzed the data; and all authors approved the final version of the manuscript.

Conflict-of-interest disclosure: N.E.L. receives consultant fees from and is on the board of directors of United States Drug Testing Laboratories. A.J.M. has received research support from Seattle Genetics, Merck, Bristol-Myers Squibb, and Incyte; and honoraria from Kyowa Hakko Kirin Pharma, Miragen Therapeutics, Takeda Pharmaceuticals, ADC Therapeutics, Seattle Genetics, Cell Medica, and Bristol-Myers Squibb. A.K. has received research support from AbbVie Pharmaceuticals, Adaptive Biotechnologies, Pharmacyclics, and Seattle Genetics; and received research support from and acted on an advisory board for Celgene and participated in steering committees for AstraZeneca. S.M.H. has consulted for Aileron, ADCT Therapeutics, Merck, Corvus, Miragen, Innate Pharma, Millennium/Takeda, Portola, Affimed, Seattle Genetics, Astex, Celgene, Kyowa-Hakka-Kirin, Verastem, and Kura;

and has received research support from Forty-Seven, Aileron, ADCT Therapeutics, Corvus, Millennium/Takeda, Portola, Seattle Genetics, Celgene, Infinity/Verastem, Trillium, and Daichii. M.E.A. has received speaker and consultant fees from Biocartis and Invivoscribe. R.L.L. is on the supervisory board of Qiagen; is a scientific advisor to Loxo (previous), Imago, C4 Therapeutics, and Isoplexis, each of which include an equity interest; received research support from Prelude; receives research support from and has consulted for Celgene and Roche and has consulted for Lilly, Janssen, Astellas, Morphosys and Novartis; and received honoraria from Roche, Lilly and Amgen for invited lectures and from Gilead for grant reviews. A.D. has received personal fees from Roche, Corvus Pharmaceuticals, Physicians' Education Resource, Seattle Genetics, Peerview Institute, Oncology Specialty Group, Celgene, Novartis, Takeda and EUSA Pharma; and research support from Roche. W.X. has received research support from Stemline Therapeutics. The remaining authors declare no competing financial interests.

The current affiliation for S.H. is Laboratory of Haematology, CHU Lyon-Sud, Hospices Civils de Lyon, Pierre-Bénite, France.

The current affiliation for N.O. is Laboratory of Pathology, National Cancer Institute, National Institutes of Health, Bethesda, MD.

ORCID profiles: N.E.L., 0000-0002-0640-7114; K.P.-D., 0000-0002-4048-8376; A.D., 0000-0001-6576-5256; W.X., 0000-0001-8586-8500.

Correspondence: Wenbin Xiao, Department of Pathology, Memorial Sloan Kettering Cancer Center, 1275 York Ave, New York, NY 10065; e-mail: xiaow@mskcc.org.

References

1. Xu B, Liu P. No survival improvement for patients with angioimmunoblastic T-cell lymphoma over the past two decades: a population-based study of 1 207 cases. *PLoS One*. 2014;9(3):e92585.
2. Cairns RA, Iqbal J, Lemonnier F, et al. IDH2 mutations are frequent in angioimmunoblastic T-cell lymphoma. *Blood*. 2012;119(8):1901-1903.
3. Couronné L, Bastard C, Bernard OA. TET2 and DNMT3A mutations in human T-cell lymphoma. *N Engl J Med*. 2012;366(1):95-96.
4. Lemonnier F, Couronné L, Parrens M, et al. Recurrent TET2 mutations in peripheral T-cell lymphomas correlate with TFH-like features and adverse clinical parameters. *Blood*. 2012;120(7):1466-1469.
5. Odejide O, Weigert O, Lane AA, et al. A targeted mutational landscape of angioimmunoblastic T-cell lymphoma. *Blood*. 2014;123(9):1293-1296.
6. Palomero T, Couronné L, Khiabani H, et al. Recurrent mutations in epigenetic regulators, RHOA and FYN kinase in peripheral T cell lymphomas. *Nat Genet*. 2014;46(2):166-170.
7. Quivoron C, Couronné L, Della Valle V, et al. TET2 inactivation results in pleiotropic hematopoietic abnormalities in mouse and is a recurrent event during human lymphomagenesis. *Cancer Cell*. 2011;20(1):25-38.
8. Sakata-Yanagimoto M, Enami T, Yoshida K, et al. Somatic RHOA mutation in angioimmunoblastic T cell lymphoma. *Nat Genet*. 2014;46(2):171-175.
9. Wang C, McKeithan TW, Gong Q, et al. IDH2R172 mutations define a unique subgroup of patients with angioimmunoblastic T-cell lymphoma. *Blood*. 2015;126(15):1741-1752.
10. Yoo HY, Sung MK, Lee SH, et al. A recurrent inactivating mutation in RHOA GTPase in angioimmunoblastic T cell lymphoma. *Nat Genet*. 2014;46(4):371-375.
11. Genovese G, Kähler AK, Handsaker RE, et al. Clonal hematopoiesis and blood-cancer risk inferred from blood DNA sequence. *N Engl J Med*. 2014;371(26):2477-2487.
12. Jaiswal S, Fontanillas P, Flannick J, et al. Age-related clonal hematopoiesis associated with adverse outcomes. *N Engl J Med*. 2014;371(26):2488-2498.
13. Xie M, Lu C, Wang J, et al. Age-related mutations associated with clonal hematopoietic expansion and malignancies. *Nat Med*. 2014;20(12):1472-1478.
14. Busque L, Patel JP, Figueroa ME, et al. Recurrent somatic TET2 mutations in normal elderly individuals with clonal hematopoiesis. *Nat Genet*. 2012;44(11):1179-1181.

15. Abdel-Wahab O, Mullally A, Hedvat C, et al. Genetic characterization of TET1, TET2, and TET3 alterations in myeloid malignancies. *Blood*. 2009;114(1):144-147.
16. Ley TJ, Ding L, Walter MJ, et al. DNMT3A mutations in acute myeloid leukemia. *N Engl J Med*. 2010;363(25):2424-2433.
17. Papaemmanuil E, Gerstung M, Malcovati L, et al; Chronic Myeloid Disorders Working Group of the International Cancer Genome Consortium. Clinical and biological implications of driver mutations in myelodysplastic syndromes. *Blood*. 2013;122(22):3616-3627, quiz 3699.
18. Cheminant M, Bruneau J, Kosmider O, et al. Efficacy of 5-azacytidine in a TET2 mutated angioimmunoblastic T cell lymphoma. *Br J Haematol*. 2015;168(6):913-916.
19. Tiacci E, Venanzi A, Ascani S, et al. High-risk clonal hematopoiesis as the origin of AITL and NPM1-mutated AML. *N Engl J Med*. 2018;379(10):981-984.
20. Tobiasson M, Pandzic T, Cavelier L, Sander B, Wahlin BE. Angioimmunoblastic T-cell lymphoma and myelodysplastic syndrome with mutations in *TET2*, *DNMT3* and *CUX1* - azacitidine induces only lymphoma remission. *Leuk Lymphoma*. 2019;60(13):3316-3319.
21. Nürnberg B, Beer-Hammer S. Function, regulation and biological roles of PI3K γ variants. *Biomolecules*. 2019;9(9):E427.
22. Tate JG, Bamford S, Jubb HC, et al. COSMIC: the Catalogue Of Somatic Mutations In Cancer. *Nucleic Acids Res*. 2019;47(D1):D941-D947.
23. Cybulski C, Górski B, Huzarski T, et al. CHEK2 is a multiorgan cancer susceptibility gene. *Am J Hum Genet*. 2004;75(6):1131-1135.
24. Buscariet M, Provost S, Zada YF, et al. *DNMT3A* and *TET2* dominate clonal hematopoiesis and demonstrate benign phenotypes and different genetic predispositions. *Blood*. 2017;130(6):753-762.
25. Acuna-Hidalgo R, Sengul H, Steehouwer M, et al. Ultra-sensitive sequencing identifies high prevalence of clonal hematopoiesis-associated mutations throughout adult life. *Am J Hum Genet*. 2017;101(1):50-64.
26. Gibson CJ, Lindsley RC, Tchekmedyian V, et al. Clonal hematopoiesis associated with adverse outcomes after autologous stem-cell transplantation for lymphoma. *J Clin Oncol*. 2017;35(14):1598-1605.
27. Kommalapati A, Tella SH, Go RS, Bennani NN, Goyal G. A population-based analysis of second primary malignancies in T-cell neoplasms. *Br J Haematol*. 2019;185(2):338-342.
28. In: Swerdlow S, Campo E, Harris N, eds., et al. *WHO Classification of Tumours of Haematopoietic and Lymphoid Tissues*, Revised 4th ed. Lyon, France: International Agency for Research on Cancer; 2017:
29. Holst JM, Plesner TL, Pedersen MB, et al. Myeloproliferative and lymphoproliferative malignancies occurring in the same patient: a nationwide discovery cohort. *Haematologica*. 2019;haematol.2019.225839.
30. Saillard C, Guermouche H, Derrieux C, et al. Response to 5-azacytidine in a patient with TET2-mutated angioimmunoblastic T-cell lymphoma and chronic myelomonocytic leukaemia preceded by an EBV-positive large B-cell lymphoma. *Hematol Oncol*. 2017;35(4):864-868.